

Supporting Information

Boosting Oxygen Reduction Reaction with Metal

Phthalocyanines: Altering Central Metals and Substituents

Kunyu Li¹, Pai Wang¹, Jiarui Li¹, Yang Gao^{1,*}, and Yanning Zhang^{1,2*}

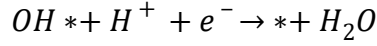
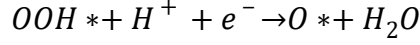
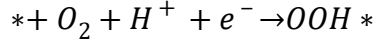
¹Institute of Fundamental and Frontier Sciences, University of Electronic Science and Technology of China, Chengdu 611731, China

²Key Laboratory for Quantum Physics and Photonic Quantum Information, Ministry of Education, University of Electronic Science and Technology of China, Chengdu 611731, China

*Correspondence to: ygaoxs@gmail.com; yanningz@uestc.edu.cn

Supplementary Note 1. Computational details.

The four-electron ORR mechanism in acidic medium was assumed as the following steps:



where *, OOH*, O* and OH* stand for an active site, adsorbed OOH* intermediate, adsorbed O* intermediate and adsorbed OH* intermediate, respectively.

The binding energies (ΔE_{ads}) of OOH*, O* and OH* were calculated by:

$$\Delta E_{ads}(OOH^*) = E_{MPC-OOH^*} - E_{MPC} - (2E_{H_2O} - 3/2E_{H_2})$$

$$\Delta E_{ads}(O^*) = E_{MPC-O^*} - E_{MPC} - (E_{H_2O} - E_{H_2})$$

$$\Delta E_{ads}(OH^*) = E_{MPC-OH^*} - E_{MPC} - (E_{H_2O} - 1/2E_{H_2})$$

where $E_{MPC-OOH^*}$, E_{MPC-O^*} , E_{MPC-OH^*} present the ground state electronic energies of OOH*, O* and OH* intermediates adsorbed on MPC, respectively. E_{H_2O} and E_{H_2} are the calculated DFT energies of isolated H₂O and H₂ molecules.

Then the Gibbs free energies of adsorption (ΔG_{ads}) can be calculated by:

$$\Delta G_{ads} = \Delta E_{ads} + \Delta ZPE - T\Delta S + \Delta G_U + \Delta G_{pH}$$

where ΔZPE denotes the corrections of zero-point energy, and $T\Delta S$ indicates the corrections of entropy. T is set as 298.15 K. ΔG_U presents the influence of the Gibbs free energies related to electrode potential U. ΔG_{pH} is the change of Gibbs free energies based on the concentration of H^+ , $\Delta G_{pH} = k_B \times \ln_{10}[H^+] = k_B \times pH \times \ln 10$, where k_B is the Boltzmann constant, and pH of an acidic medium is assumed be zero.

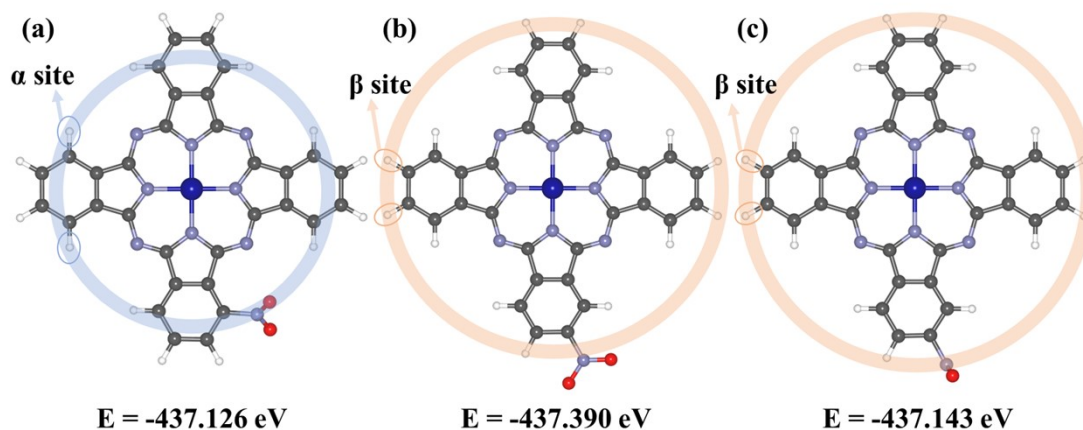


Figure S1. Structures of (a) the substituent positioned at the α site, (b) the substituent positioned at the β site, and (c) the substituent perpendicular to the macrocycle.

For the positioning of the substituents (see **Figure S1**), using NO_2 substituents as an example, our energy calculations show that the β sites (**Figure S1 (b)**) are energetically more favorable than the α sites (**Figure S1 (a)**) by 0.264 eV. This energy difference indicates a higher likelihood of substituents being located at the β sites. Accordingly, we have specified in the manuscript that the substituents are positioned at the β sites.

Furthermore, we conducted an analysis comparing the stability of different configurations of the substituents relative to the macrocycle. Our findings indicate that when the substituents are in equilibrium with the macrocycle (**Figure S1 (b)**), the energy is 0.247 eV lower than when the substituents are perpendicular to the macrocycle (**Figure S1 (c)**). This suggests that the substituents are most stable when located at the β sites and in equilibrium with the macrocycle, supporting the proposed configuration.

Table S1. Free energies of adsorption of oxygenated intermediates on MPcs and cobalt phthalocyanine complexes.

| ΔG_{ads} (eV) | $\Delta G_{(\text{OOH}^*)}$ | $\Delta G_{(\text{O}^*)}$ | $\Delta G_{(\text{OH}^*)}$ |
|---|-----------------------------|---------------------------|----------------------------|
| CrPc | 3.49 | 0.54 | 0.19 |
| MnPc | 3.86 | 1.38 | 0.60 |
| FePc | 3.94 | 1.48 | 0.78 |
| CoPc | 4.22 | 2.76 | 1.18 |
| NiPc | 4.89 | 4.37 | 2.18 |
| CoPc(NO₂)₄ | 4.05 | 2.84 | 1.22 |
| CoPc(NO₂)₃(NH₂)₁ | 4.06 | 2.81 | 1.22 |
| CoPc(NO₂)₂(NH₂)₂ | 4.06 | 2.79 | 1.21 |
| CoPc(NO₂)₁(NH₂)₃ | 4.15 | 2.73 | 1.17 |
| CoPc (NH₂)₄ | 4.20 | 2.70 | 1.14 |

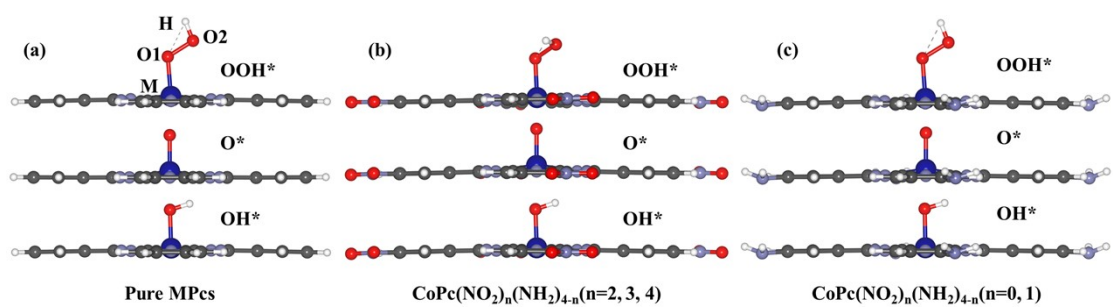


Figure S2 Structures of intermediates on (a) pure MPcs, (b) $\text{CoPc}(\text{NO}_2)_n(\text{NH}_2)_{4-n}$ ($n=2, 3, 4$) and (c) $\text{CoPc}(\text{NO}_2)_n(\text{NH}_2)_{4-n}$ ($n=0, 1$).

Table S2. Summary of structural parameters for intermediates on MPcs and their complexes.

| MPc | intermediates | M-O1 bond (Å) | O1-O2 bond (Å) | O2-H bond (Å) |
|---|---------------|---------------|----------------|---------------|
| CrPc | OOH* | 1.821 | 1.481 | 0.979 |
| | O* | 1.561 | | |
| | OH* | 1.826 | | 0.975 |
| MnPc | OOH* | 1.966 | 1.452 | 0.978 |
| | O* | 1.586 | | |
| | OH* | 1.918 | | 0.973 |
| FePc | OOH* | 1.919 | 1.440 | 0.979 |
| | O* | 1.642 | | |
| | OH* | 1.788 | | 0.980 |
| CoPc | OOH* | 1.897 | 1.429 | 0.981 |
| | O* | 1.734 | | |
| | OH* | 1.840 | | 0.978 |
| NiPc | OOH* | 2.202 | 1.393 | 0.984 |
| | O* | 1.936 | | |
| | OH* | 2.016 | | 0.977 |
| CoPc(NO₂)₄ | OOH* | 1.858 | 1.408 | 0.984 |
| | O* | 1.733 | | |
| | OH* | 1.838 | | 0.978 |
| CoPc(NO₂)₃(NH₂)₁ | OOH* | 1.856 | 1.411 | 0.984 |
| | O* | 1.733 | | |
| | OH* | 1.840 | | 0.978 |
| CoPc(NO₂)₂(NH₂)₂ | OOH* | 1.857 | 1.413 | 0.983 |
| | O* | 1.733 | | |
| | OH* | 1.841 | | 0.978 |
| CoPc(NO₂)₁(NH₂)₃ | OOH* | 1.905 | 1.430 | 0.981 |
| | O* | 1.733 | | |

| | | | | |
|---|------|-------|-------|-------|
| | OH* | 1.842 | | 0.978 |
| | OOH* | 1.896 | 1.436 | 0.980 |
| CoPc(NH₂)₄ | O* | 1.733 | | |
| | OH* | 1.844 | | 0.978 |

Structural diagrams of the intermediates are presented in **Figure S2** and **Table S2**. The data show that the M-O1 bond lengths in CoPc(NO₂)_n(NH₂)_{4-n} (n = 2, 3, 4) are approximately 1.857 Å, 1.733 Å, and 1.840 Å when adsorbed with OOH*, O*, and OH*, respectively. For other MPcs, the M-O1 bond lengths range between 1.821 and 2.202 Å with OOH* adsorption, between 1.561 and 1.936 Å with O* adsorption, and between 1.788 and 2.016 Å with OH* adsorption. These results suggest that CoPc(NO₂)_n(NH₂)_{4-n} (n = 2, 3, 4) exhibits moderate M-O1 bond lengths compared to other MPcs, which are more favorable for the electrochemical reaction process.

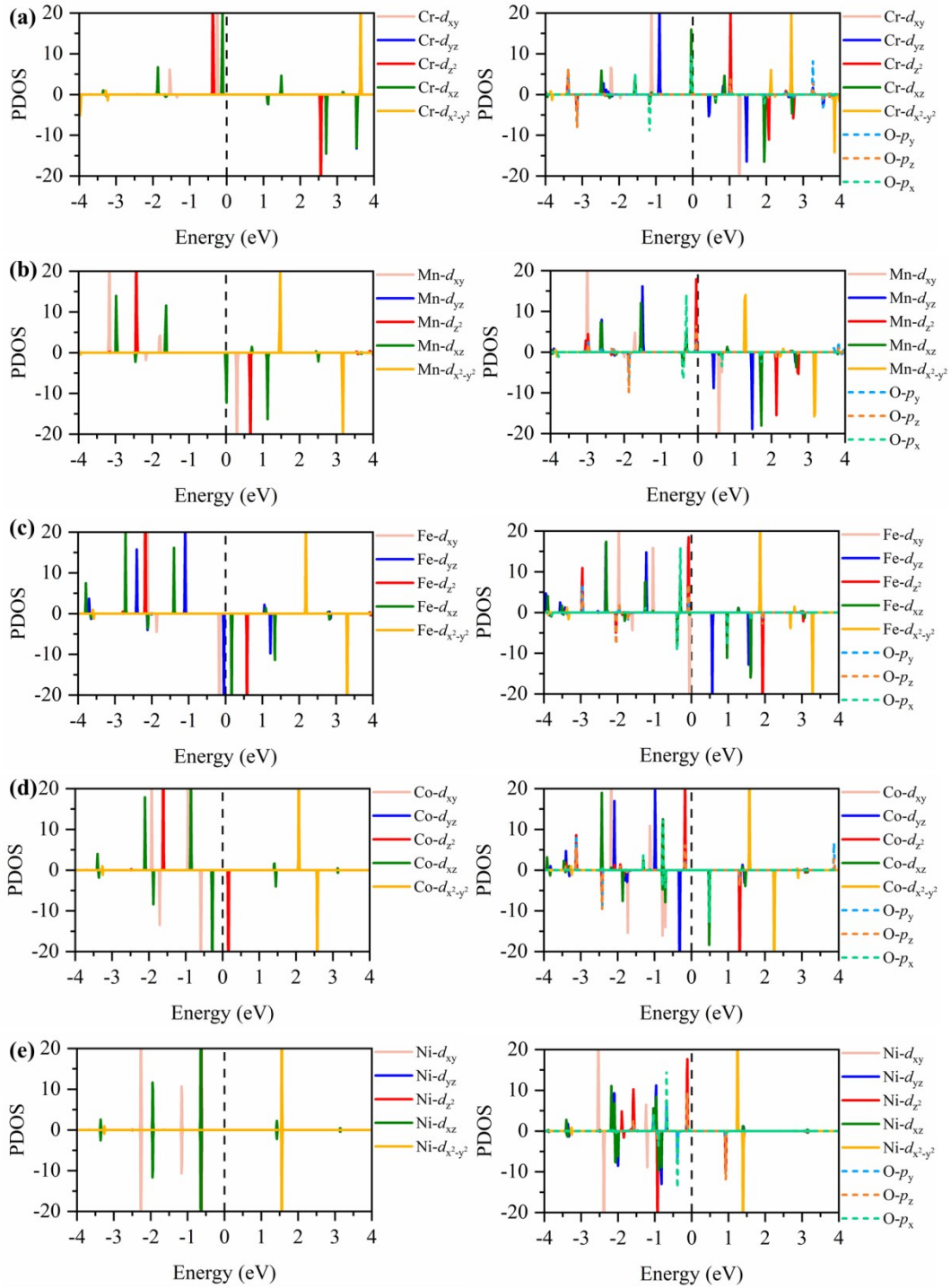


Figure S3. (a-e) Projected density of states (PDOS) for Mpc and OOH* adsorbed on Mpc. (M=Cr, Mn, Fe, Co, Ni).

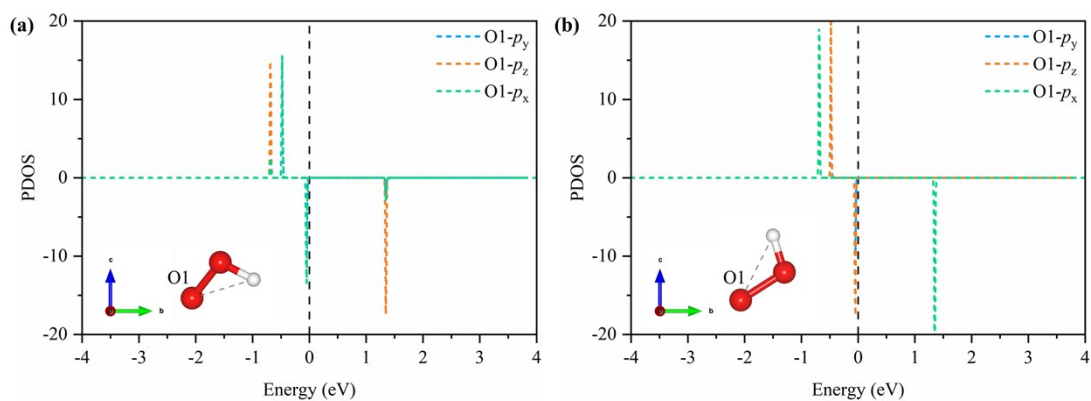


Figure S4. PDOS of OOH molecule in (a) Cycle I and (b) Cycle II.

For Cycle I, our calculations reveal that the p_z orbital of the OOH molecule is distinct in energy from the p_x and p_y orbitals, which remain degenerate. In contrast, in Cycle II, the p_x orbital is no longer degenerate with the other p orbitals, while the p_y and p_z orbitals exhibit degeneracy. These findings indicate that the orbital degeneracies in the OOH molecule are sensitive to the initial configuration and the orientation of the coordinate axes. Depending on whether the configuration corresponds to Cycle I or Cycle II, one p orbital may not degenerate, while the other two p orbitals exhibit degeneracy.

Table S3. ICOHP values for Metal-O bond of OOH* adsorbed on different MPcs.

| MPcs | CrPc | MnPc | FePc | CoPc | NiPc |
|---|-------------|-------------|-------------|-------------|-------------|
| ICOHP-UP | -2.584 | -1.775 | -1.767 | -1.573 | -1.133 |
| d_z^2-p_z(up) | -0.629 | -0.234 | -0.196 | -0.061 | -0.043 |
| d_{xz}-p_x(up) | -0.196 | -0.004 | -0.003 | 0.002 | -0.003 |
| d_{yz}-p_y(up) | -0.148 | -0.047 | -0.048 | -0.047 | -0.005 |
| ICOHP-DOWN | -2.817 | -2.589 | -2.708 | -2.699 | -1.465 |
| d_z^2-p_z(dw) | -0.549 | -0.525 | -0.561 | -0.564 | -0.323 |
| d_{xz}-p_x(dw) | -0.481 | -0.325 | -0.358 | -0.354 | -0.004 |
| d_{yz}-p_y(dw) | -0.166 | -0.082 | -0.091 | -0.069 | -0.007 |
| TOT | -5.401 | -4.364 | -4.475 | -4.272 | -2.598 |

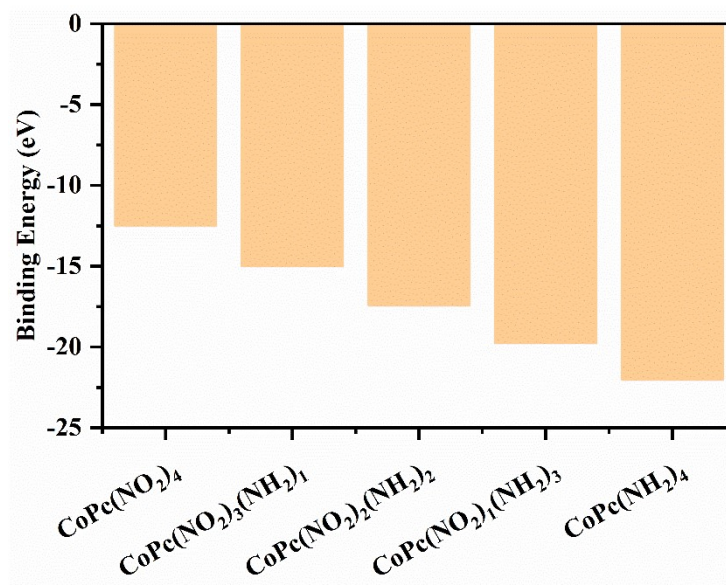


Figure S5. Calculated binding energy of cobalt phthalocyanine complexes.

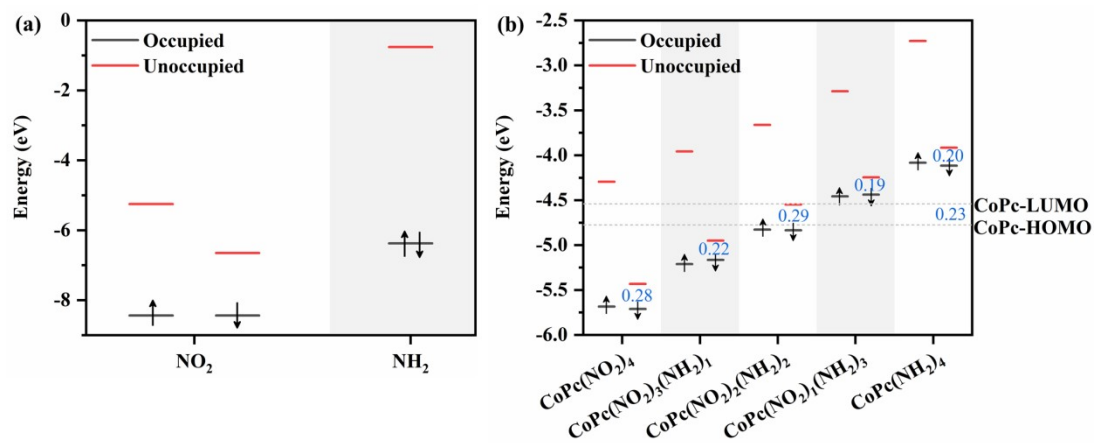


Figure S6. (a) HOMO and LUMO of isolated NO₂ and NH₂. (b) Effects of NO₂ and NH₂ on HOMO and LUMO energy on cobalt phthalocyanine complexes.

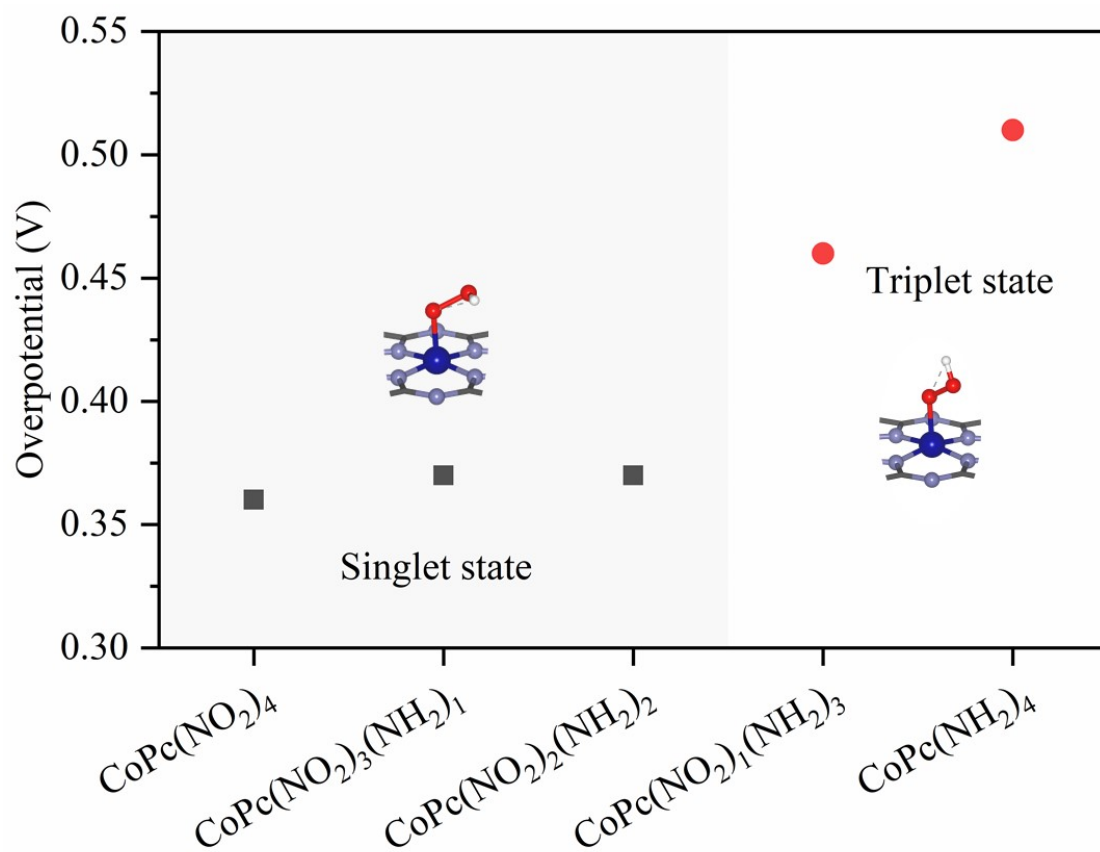


Figure S7. Overpotentials of CoPc complexes with different spin states when OOH^* adsorbed.

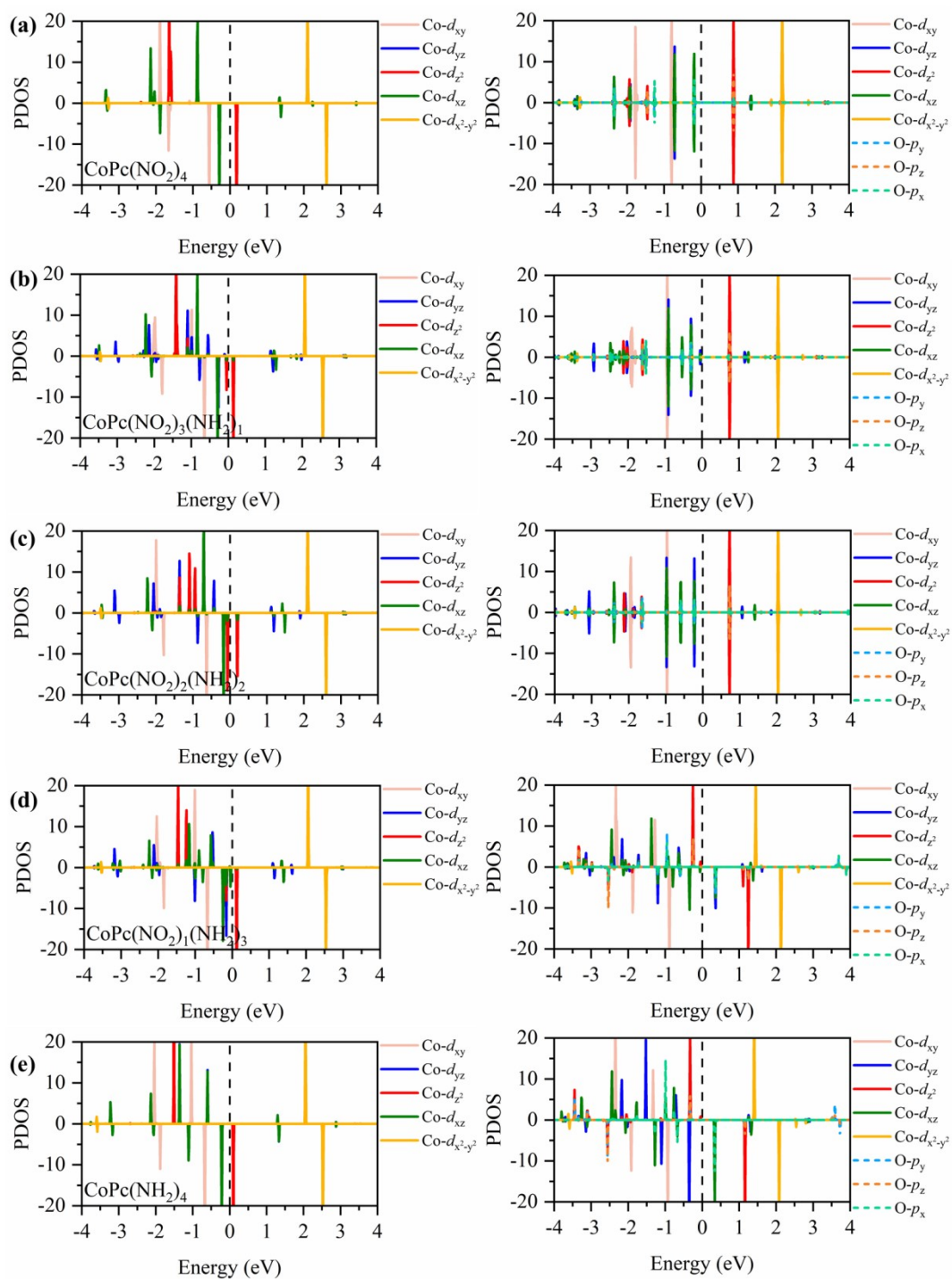


Figure S8. (a-e) Projected density of states (PDOS) for $\text{CoPc}(\text{NO}_2)_n(\text{NH}_2)_{4-n}$ ($n=0, 1, 2, 3, 4$) and OOH^* adsorbed on $\text{CoPc}(\text{NO}_2)_n(\text{NH}_2)_{4-n}$.

Table S4. ICOHP values for Co-O bond of OOH* adsorbed on different substituted cobalt phthalocyanine complexes.

| CoPc(NO₂)_n(NH₂)_{4-n} | n=4 | n=3 | n=2 | n=1 | n=0 |
|---|------------|------------|------------|------------|------------|
| ICOHP-UP | -2.483 | -2.468 | -2.444 | -1.531 | -1.549 |
| d_z²-p_z(up) | -0.640 | -0.645 | -0.647 | -0.047 | -0.052 |
| d_{xz}-p_x(up) | -0.040 | -0.044 | -0.031 | -0.026 | 0.002 |
| d_{yz}-p_y(up) | -0.051 | -0.046 | -0.044 | -0.020 | -0.048 |
| ICOHP-DOWN | -2.482 | -2.468 | -2.445 | -2.651 | -2.681 |
| d_z²-p_z(dw) | -0.640 | -0.645 | -0.647 | -0.588 | -0.567 |
| d_{xz}-p_x(dw) | -0.040 | -0.044 | -0.030 | -0.186 | -0.349 |
| d_{yz}-p_y(dw) | -0.051 | -0.046 | -0.044 | -0.223 | -0.073 |
| TOT | -4.965 | -4.936 | -4.889 | -4.183 | -4.230 |

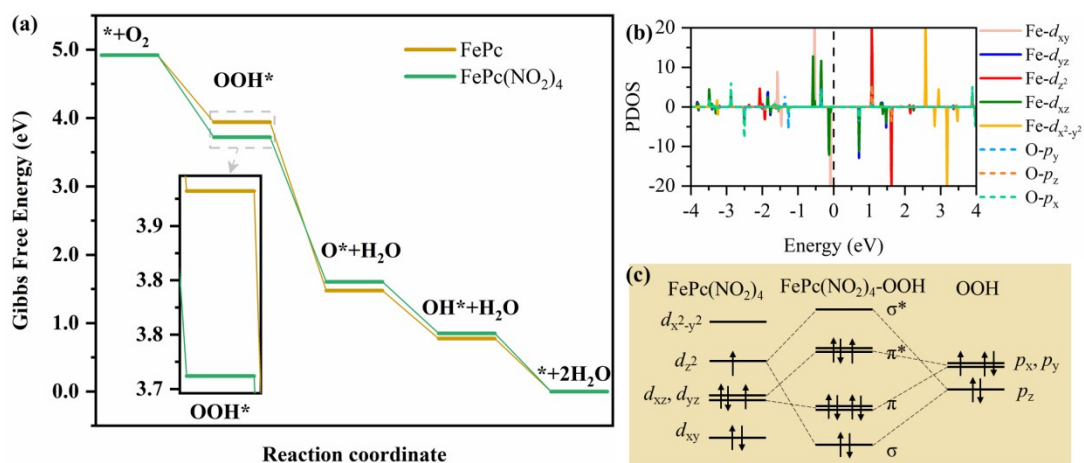


Figure S9. (a) Gibbs free energy diagrams for ORR on substituted iron phthalocyanine complexes at $U = 0$ V. (b) Projected density of states (PDOS) for OOH* adsorbed on FePc(NO₂)₄. (c) Orbital interaction between the cobalt atom of FePc(NO₂)₄ and OOH* when the OOH* adsorbed.

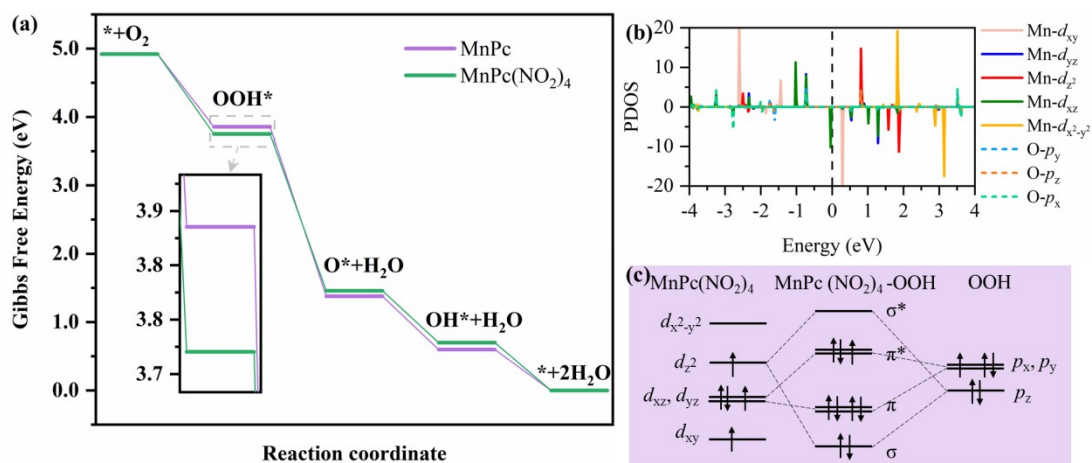


Figure S10. (a) Gibbs free energy diagrams for ORR on substituted manganese phthalocyanine complexes at $U = 0$ V. (b) Projected density of states (PDOS) for OOH* adsorbed on MnPc(NO₂)₄. (c) Orbital interaction between the cobalt atom of MnPc(NO₂)₄ and OOH* when the OOH* adsorbed.